



# **SYNTHESIS OF NEW AZO REAGENT FOR DETERMINATION OF Pd(II), Ag(I) AND APPLIED TO ENHANCE THE PROPERTIES OF SILVER NANO PARTICLES**

**AAYAD AMMAR SAYHOOD<sup>\*,a</sup> and HUSSAIN J. MOHAMMED**

Department of Chemistry, Faculty of Science, University of Kufa, AL-NAJAF 54001, IRAQ

<sup>a</sup>Department of Basic Sciences, Faculty of Dentistry, University of Kufa, AL-NAJAF 54001, IRAQ

## **ABSTRACT**

This study describes the use of novel azo dye reagent, (L), (E)-5-(4-[(1,5-dimethyl-3-oxo-2-phenyl-2, 3-dihydro-1H-pyrazol-4-yl)diazanyl]phenyl)-5-ethylpyrimidine-2,4,6 (1H, 3H, 5H)-trione, have been synthesized between phenolphthalein with 4-aminoantipyrine and characterized by IR, <sup>1</sup>H NMR, <sup>13</sup>C NMR spectra and CHNO analysis, as simple, selective and reliable analytical reagent for the determination of Pd(II) and Ag(I) ions spectrophotometrically. The reagent reacts with ions at pH 4 for Pd(II) and 8 for Ag(I) and formed colored complexes 1:1 stoichiometry of Pd(II) and Ag(I), which show a maximum absorbance of 518 and 492 nm of molar ratio absorptivity  $5.331 \times 10^3$  and  $1.025 \times 10^4$  L.mol<sup>-1</sup> cm<sup>-1</sup>, respectively. Fixed optimum conditions were constructed, precision, accuracy, R. S. D. and effect of solvents. The Beer's law was obeyed 0.1-3 mg/L. The reagent was used for enhance the properties of nano silver by ligand exchange reaction on nanoparticles.

**Key words:** Azo dye reagent, Spectrophotometric, Phenolphthalein, Effect of solvents, Nano silver.

## **INTRODUCTION**

In recent years, azo compounds got the attention of a large number of scientists and researchers, which is considered a very important class of chemical compounds they containing a heterocyclic moiety<sup>1</sup>. This interest represents through the synthesis of a large number of common uses of these compounds in the field determination of ions<sup>2</sup>, dyes<sup>3</sup>, biological<sup>4</sup> and pharmacological activities<sup>5</sup>. Characterized azo compounds containing N, O donor atoms have the ability to configure the complexes with transition and non-transition metal ions<sup>6</sup>, which synthesized by coupling a diazonium reagent with an aromatic compound<sup>7</sup>. Which gives colored compounds with stable chemical and physical properties<sup>8</sup>. 4-aminoantipyrine was considered one of the most important derivatives of these

---

\* Author for correspondence; E-mail: ayad.alzaidi@uokufa.edu.iq

compounds<sup>9</sup>. The coordination property of 4-aminoantipyrine ligand has been changed to stretch a flexible, formed by condensation with variation reagents like ketones and aldehydes<sup>10</sup>. Silver nanoparticles attracted significant attention due their applications in optics their use as substrate for surface enhanced Raman spectroscopy (SERS)<sup>11</sup> and in biological field as antibacterial agents<sup>12</sup>. In this paper, the synthesis of new organic reagent based on 4-aminoantipyrine interaction with the drug substance phenoparpetal to determine the palladium and silver ions in the solutions after apply their optimal conditions, the new reagent was used to improve the qualities of silver nanoparticles.

## EXPERIMENTAL

### Materials and apparatus

All chemicals of highest purity were used in this work, which were supplied by Fluka and BDH. Spectrophotometric measurements were made with Shimadzu UV-Visible 1650 PC double beam. The FTIR measurements were made in Shimadzu 8400 Series Japan. <sup>1</sup>H NMR spectra were measured on BRUKER AV 400 Avance-III 400 MHz instrument. <sup>13</sup>C NMR spectra were measured on BRUKER AV 100 Avance-III 100 MHz instrument. CE 440 CHN/O/S elemental analyser was made by EAI. Scanning electron microscope (SEM) Inspect S50 for materials science/EFI. AA2000 Atomic force microscope (AFM) Angstrom advanced. VCX 130 PB-VCX 130 FSJ/Sonics vibra cell ultrasonic. The pH measurements were performed with HANNA pH meter H19811-5 instrument.

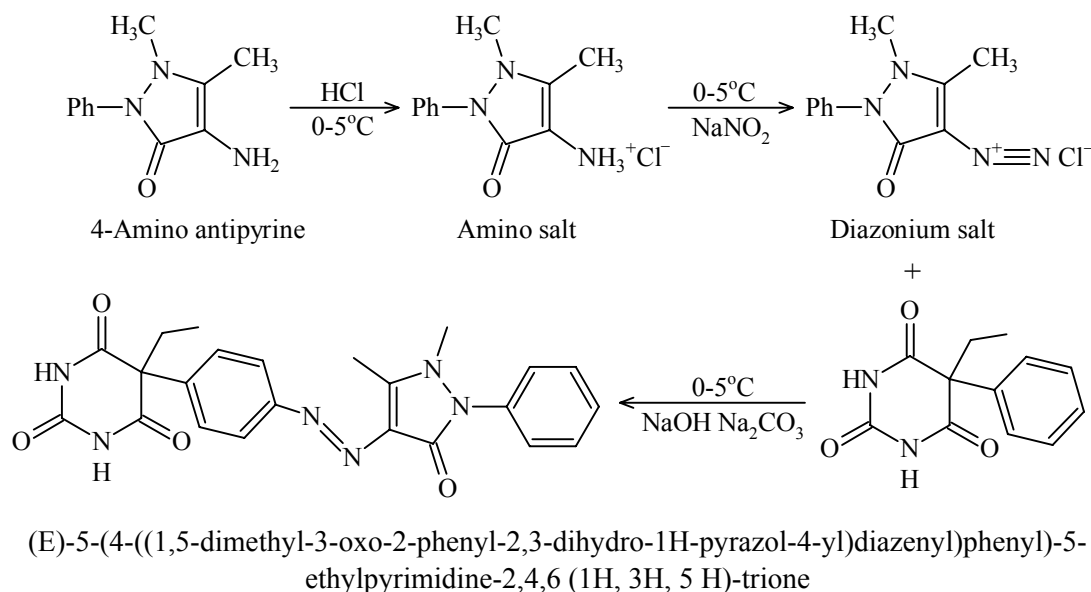
### Synthesis of reagent

The reaction of the formation of azo ligand (L) from 4-aminoantipyrine is shown in the Scheme 1. The reagent and solvent were of analytical grade and used without further purification. 4-Aminoantipyrine (0.00492 mole) 1.00 g was diazotized by dissolving it in 25 mL ethanol, then 5 mL of concentrated HCl was adding keeping the temperature at 0-5°C and then adding NaNO<sub>2</sub> solution gradually and left the solution about 15 min. The diazonium salt was spontaneously added slowly drop wise to a well cooled alkaline solution of coupling agent (phenoparpetal 1.1424 g), the mixture was allowed to stand for 1 hr. The dark colored mixture was neutralized with HCl and the solid precipitate was filtered off and washed several times with (1:1) (ethanol : water) mixture then recrystallised from boiling methanol and left to dry (**Scheme 1**).

### Solutions

- A stock standard palladium solution (100 mg/L) was prepared by dissolving 0.0353 g of PdCl<sub>2</sub>, the volume was completed to 200 mL with distilled water in the presence of 5 M of hydrochloric acid.

- A stock standard silver solution (100 mg/L) was prepared by dissolving 0.0314 g of AgNO<sub>3</sub>, the volume was completed to 200 mL with distilled water.
- Solution of azo dye reagent ( $1 \times 10^{-3}$  M) were prepared by dissolving (0.0516 g) and complete the volume to 100 mL with absolute methanol.



**Scheme 1: Mechanism of preparation of the ligand**

## RESULTS AND DISCUSSION

### Absorption spectra

The electronic spectra of reagent and their complexes with Pd(II) and Ag(I) ions were fixed in (Fig. 1). The UV-Vis spectra of the ligand under investigation display mainly three peaks observed in ethanol within the range 200-800 nm. The first and two peaks are in the region 247, 294 nm were assigned to the moderate energy  $\pi \rightarrow \pi^*$  transition of the aromatic rings. The third broad peak ( $\lambda_{\text{max}}$ ) in the range 447 nm was related to the  $n \rightarrow \pi^*$  transition of intermolecular charge-transfer taken place through the azo group (N=N observed as a shoulder may be attributed to the  $n \rightarrow \pi^*$  transition resulted from the presence of groups containing a double bond), the interaction between the metal ion and the ligand manifests itself in the absorption spectra by the appearance of one absorption band with maxima in the range 492-520 nm. A great bathochromic shift in the visible region was detected in the complex solution spectra with respect to that of the free ligand.

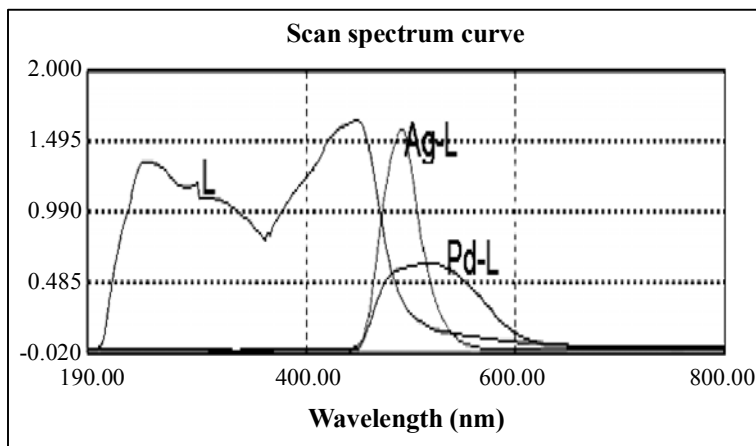


Fig. 1: The absorbance  $\lambda_{\max}$  of reagent and their complexes

### FTIR spectra and elemental analysis

The FTIR data of reagent and their complexes are given in Table 1. Here some important bands are observed in the spectra of the complexes while comparing with (L), which is helpful in detection of donation sites. The IR spectra of the free ligand have a broad band around  $3495.0 \text{ cm}^{-1}$ , which could be attributed to O-H stretching vibration and it shifted to lower frequency. The stretching frequency of carbonyl group of ligand  $\nu(\text{C}=\text{O})$  at  $1676.14 \text{ (s) cm}^{-1}$  is shifted to a lower frequency range in complexes. Similarly, the frequency corresponding to  $\nu(\text{N}=\text{N})$  at  $1492.9 \text{ cm}^{-1}$  shifted range ( $1454\text{-}11489 \text{ cm}^{-1}$ ) in complexes.

Table 1: The most important band and their assignments of L1 and their complexes ( $\text{cm}^{-1}$ )

Compd.	$\nu \text{ OH}$	$\nu \text{ C-H}$ Aromatic	$\nu \text{ C=O}$	$\nu \text{ N=N}$ CNNC	$\nu \text{ CN=NC}$	$\nu \text{ (M-O)}$	$\nu \text{ (M-N)}$
Reagent	3495.0	3157.47	1676.14	1535.34 1492.90	1132.21 1103.28	–	–
Pd-L	3402.54	3242.42	1670.41	1535.3 1489.1	1132.2 1111.03	497.65	449.43
Ag-L	3441.12	3070.78	1680.05	1491.02 1454.38	1136.11 1118.75	511.15	498

The shifting in wave number and their intensities of referenced bands led to predict the chelation behavior, i.e., coordination occurs through ring carbonyl oxygen atom and with

the nitrogen atom of azo group. The spectra of metal complexes also show additional bands in (497-511)  $w\text{ cm}^{-1}$  and (449-498)  $w\text{ cm}^{-1}$ , which is probably due to the formation of  $\nu(\text{M-O})$  and  $\nu(\text{M-N})$  bond, respectively<sup>13</sup>. Elemental analysis (%): Anal. Calc. for  $\text{C}_{23}\text{H}_{22}\text{N}_6\text{O}_4$ : C, 61.87; H, 4.97; N, 18.82; O 14.33 and found: C, 61.80; H, 4.91; N, 18.74; O 14.28.

### <sup>1</sup>H NMR and <sup>13</sup>C-NMR Studies

The <sup>1</sup>H NMR and <sup>13</sup>C-NMR spectra of the Ligand (L) in DMSO solution shows the following signals (Fig. 2-4). The <sup>1</sup>H NMR spectra shows a multiplet at  $\delta$  7.2 to 7.6 ppm (m, 6H, Ar) are due to phenyl group, -N-CH<sub>3</sub> at  $\delta$  3.4 ppm (s, 3H), =C-CH<sub>3</sub> at  $\delta$  2.7 ppm CH<sub>2</sub>-CH<sub>3</sub> at  $\delta$  (0.9-1.028) ppm, CH<sub>2</sub> at  $\delta$  (2.466-2.521) ppm NH at  $\delta$  (8.5) ppm. The <sup>13</sup>C NMR spectrum of Ligand shows the following signals (Fig. 5-7) 127-130 ppm (13C, Ar-C); 145 ppm (C=O); 30 ppm (C-CH<sub>3</sub>); 52 ppm (N-CH<sub>3</sub>), 121-128 ppm (C-N-C=N). The <sup>1</sup>H NMR and <sup>13</sup>C-NMR spectra of the complexes are shown in Table 2-3.

**Table 2: The <sup>1</sup>H NMR of reagent and their complexes**

Assignments	L1	Pd(II)	Ag(I)
C-CH <sub>3</sub>	2.7	2.19	2.08
N-CH <sub>3</sub>	3.4	3.415	3.2
H aromatic	7.2 to 7.6	7.27-7.61	7.34-7.55
CO-M	–	4.666	4.3
CH <sub>2</sub> -CH <sub>3</sub>	0.9-1.028	1.26-1.67	1.1-1.3
CH <sub>2</sub>	2.466-2.521	3.05-3.3	3.1-3.2
N-H	8.5	–	

**Table 3: The <sup>13</sup>C-NMR spectrum of reagent and their complexes**

Assignments	L1	Pd(II)	Ag(I)
C-CH <sub>3</sub>	30	25.21	24
N-CH <sub>3</sub>	52	52.17	40.56
<sup>13</sup> C, Ar-C	127-133	127-130	122-133
CO	–	102.5	102.19
C=O	145	167	160



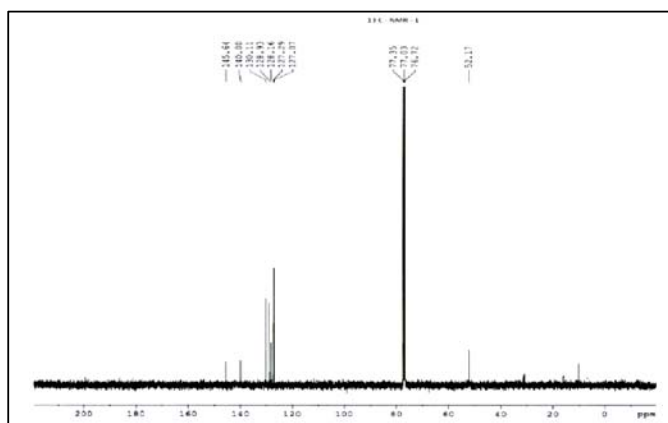


Fig. 5: The <sup>13</sup>C NMR spectra of the reagent (L)

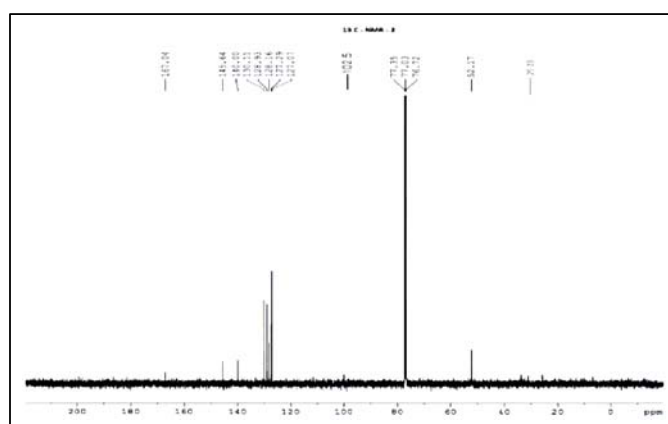


Fig. 6: The <sup>13</sup>C NMR spectra of the Pd-L

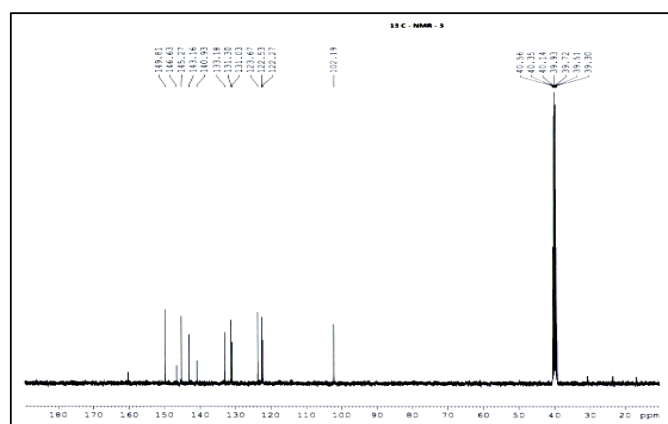


Fig. 7: The <sup>13</sup>C NMR spectra of the Ag-L

### Construction of calibration curve

At optimum conditions, a linear calibration graph for Pd-L and Ag-L were obtained, that beers law is obeyed over the concentration range of (0.1-3 mg/L) Pd(II) and Ag(I) with  $R^2$  equal to (0.9968) and (0.9974), the Sandell sensitivity is equal to 0.0199 and 0.0105, the molar ratio absorbitivity is  $5.331 \times 10^3$  and  $1.025 \times 10^4$ , respectively. The results of analytical performance are summarized in Table 4.

**Table 4: Analytical characteristics of metal-L complexes**

Characteristic	Pd(II)	Ag(I)
Absorption maxima ( $\lambda_{\max}$ ) nm	518	492
Bee's law range ( $\mu\text{g/mL}$ )	0.1-3	0.1-3
Molar absorptivity ( $\text{L}\cdot\text{mol}^{-1}\text{cm}^{-1}$ )	$5.331 \times 10^3$	$1.025 \times 10^4$
Sandell's sensitivity ( $\mu\text{g cm}^2$ )	0.0199	0.0105
pH	4	8
Stability constant	$2.8 \times 10^7$	$4.92 \times 10^6$

### Effect of pH

The UV-Vis spectra were measured for a set of mixed solutions have different pH value (Fig. 8) by using of HCl and NaOH (0.05 M) solutions (pH 2-10).

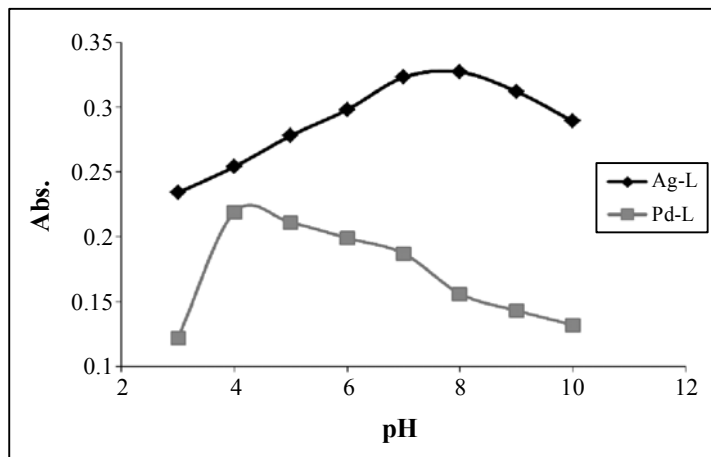


**Fig. 8: Effect of pH**



The curves show high intensity of color at pH 4 for Pd(II) and pH 8 for Ag(I) represent the completion of the reaction. At the same time, the descending part of the curves may represent the dissociation of the formed complexes at highly basic medium. However, it is well known that most of the chelate complexes are formed in neutral or basic medium.

### Effect of time

The stability of complexes with time at 518 and 492 for Pd(II) and Ag(I) are shown in (Fig. 9), After mixing the components, the absorbance reaches its maximum within 1 min at room temperature and remains stable for at least 24 hr.

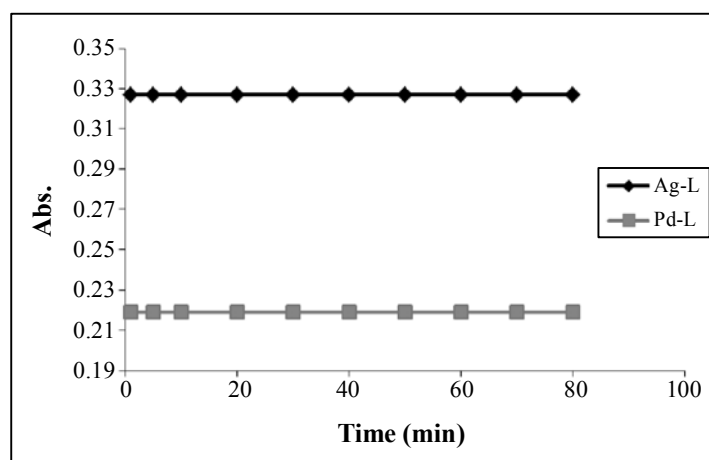


Fig. 9: The effect of time

### Accuracy and precision

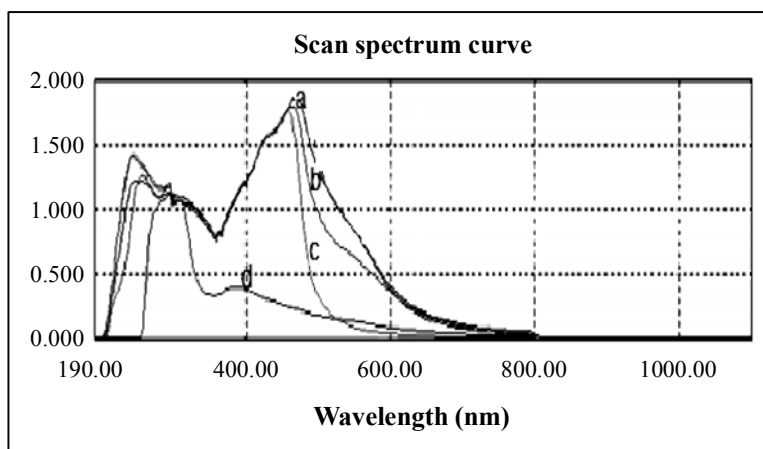
To determine the accuracy and precision of the method, Pd(II) and Ag(I) were determined at 0.1 M concentrations. The results shown in Table 5 shows satisfactory precision and accuracy with the proposed method.

Table 5: Accuracy and precision values of complexes

Ions	Conc. (mg/L)	R.S.D. (%)	Error (%)	D. L. (mg/L)
Pd(II)	1.0	0.727667818	0.4545	0.0109232
Ag(I)	1.0	0.388009529	0.3	0.00582

### Study of the absorption spectrum of reagent using different solvents

Fig. 10 shows the absorbance spectrum of reagent in different solvents. There were differences of  $\lambda_{\max}$  for reagent in different solvents. Since all the solvents used in this work were polar in nature (DMSO, ethanol, methanol and propanol) one would expect that the dye would bind more strongly to a more polar solvent and thus cause the spectra to shift to lower wavelengths, the  $\lambda_{\max}$  value is shifted to lower energies in highly polar solvents as shown in DMSO because of strong solvent-solvent interaction or the specific interaction between the solvent and hydrogen from the NH group in the dye molecule. The dye interaction becomes different with increasing capability of a given solvent to form H bonds in solution.



**Fig. 10: Study of the absorption spectrum of reagent using different solvents (a: DMSO/ b: Methanol/ c: Ethanol d: propanol)**

### Study of the absorption spectrum of reagent using of a mixture of solvents

In this study, we test the solubility of reagent by using different ratios of (DMSO/ Ethanol) mixture the ratio was (1:9, 2:8, 3:7, 4:6, 5:5, 6:4, 7:3, 8:2 and 9:1) by scanning for each solution against the blank. When absorption spectra are recorded in solvents of different polarity, it is found that the positions and intensities of the absorption bands are usually modified. Usually, the spectral shifts are attributed to specific solute-solute and solute-solvent interaction in the form of hydrogen bonding or bulk solvent properties. For the molecular systems without intramolecular hydrogen bond, the spectral shifts are sensitive to the solvent polarity. Thus, in many molecules the bands ( $\pi \rightarrow \pi^*$ ) are shifted bathochromically when the solvent polarity increases. These changes were attributed to hydrogen-bonding interaction between the solute molecule and the solvent molecule. On the other hand, the spectral shifts in the molecular systems with intramolecular hydrogen bonds

are very small. As shown in Fig. 11, the ratio 9:1 for (DMSO/Ethanol) has a higher effect on absorbance.

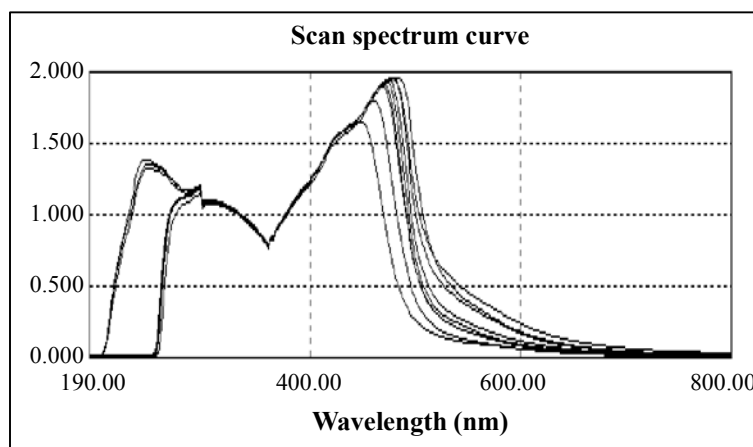


**Fig. 11: Absorption spectrum of reagent using of mixture of (DMSO/Ethanol) solvents in different ratios**

### Enhancing the properties of silver nano particles

In this paper, an application of the silver nanoparticles to ensure improved properties in terms of reducing the diameter by the ligand exchange reaction on nanoparticles<sup>12</sup>. It covers the surface of the nanoparticles compounds with ligand to prevent the aggregation of these compounds, and the bond between organic compounds and nanoparticles of physical type and this leads to occurrence of aggregation of nanoparticles compounds with the passage of time, so that enhance the stability of given nanoparticles, the molecules of ligand on the surface can be exchanged by other ligands can perhaps be responsible for new functionality or properties to the particles<sup>14</sup>. Thus, new ligand bind stronger with nanoparticles. The ligand exchange reaction on nanoparticles is the methods used for this purpose, by blending free ligand with nanoparticles compound. The purified Ag nanocrystals were dissolved in ligands and stirred at room temperature. The Ag nanocrystals were analysis by SEM and AFM. Morphology and structure<sup>15</sup>, SEM observations show that the products are very aggregate and they converted to spherical particles. This morphological change may partially because the surface silver ions, which bound to the original ligands of stearate ions, at the highly reactive sites, such as tips or corners of the nanopyramids, were stripped in the ligand exchange process. The AFM results show that the average diameters determined by the AFM are 61.77 nm and 43.70 nm for nano silver before and after the ligand exchange, respectively, as in (Fig. 12-15) before and after the ligand exchange.

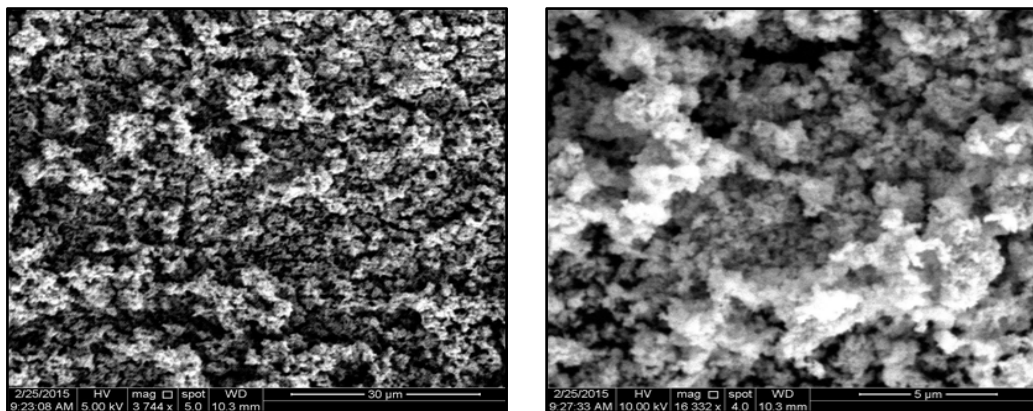


Fig. 12: Before ligand exchange by SEM

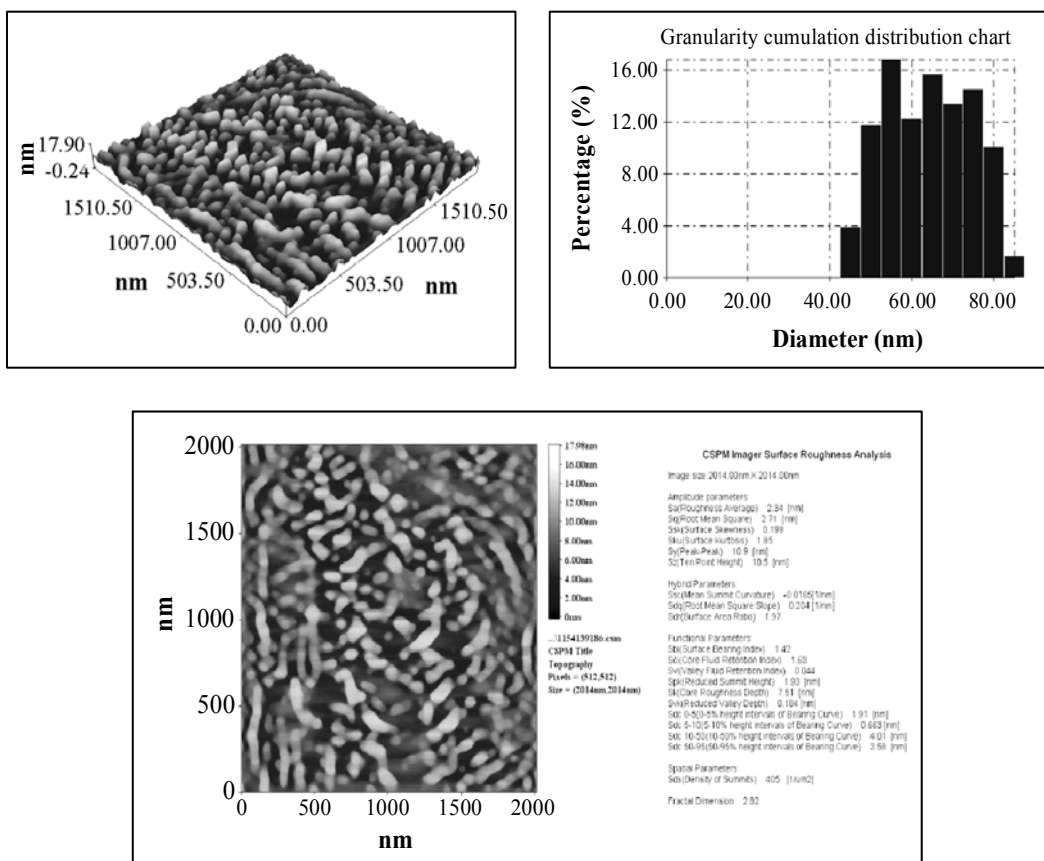


Fig. 13: Before ligand exchange by AFM

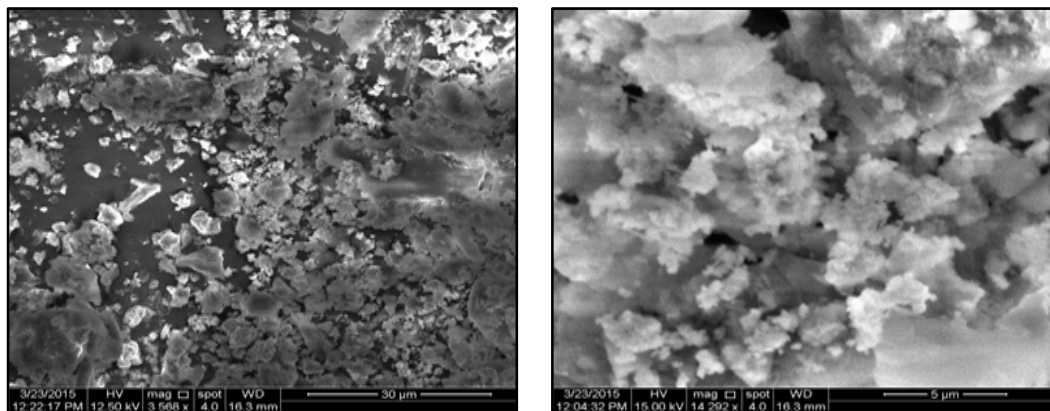


Fig. 14: After Ligand Exchange by SEM

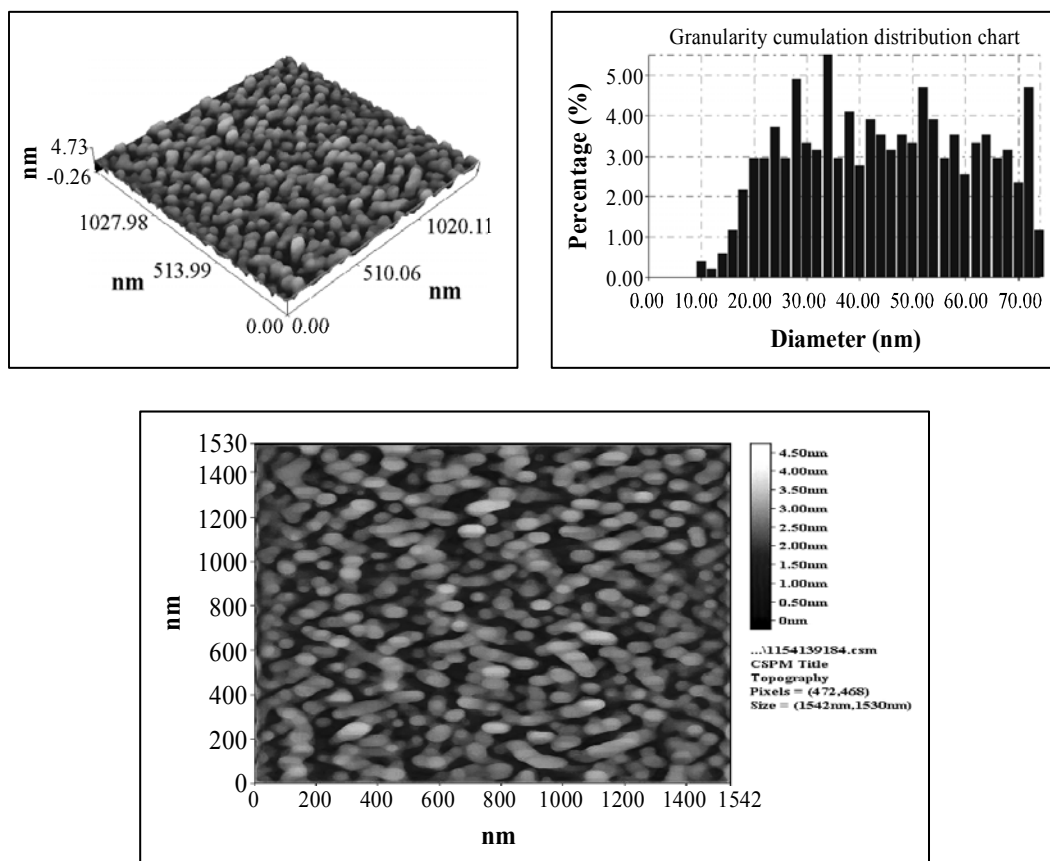


Fig. 15: After ligand exchange by AFM

## ACKNOWLEDGMENT

The authors are grateful for Mr. Safaa Abdul Hassan, Central Laboratory Service/Ibn Al-Haytham College of Education Pure Sciences/Baghdad University for his assistance.

## REFERENCES

1. B. Kirkan and R. Gup, Turkish J. Chem., **32**, 9 (2008).
2. J. J. Porter, J. L. Murray and K. B. Takvorian, J. Heterocycl. Chem., **10**, 43 (1973).
3. S. Seidenari, L. Mantovani, B. M. Manzini and M. Pignatti, Contact Dermatitis, **36**, 91 (1997).
4. V. Mkpennie, G. Ebong, I. B. Obot and B. Abasiokong, E-J. Chem., **5**, 431 (2008).
5. J. Kaszuba, L. Konieczny, B. Piekarska, I. Rotterman and J. Rybarska, J. Physiol. Pharmacol., **44**, 233 (1993).
6. C. Anitha, C. D. Sheela, P. Tharmaraj and R. Shanmugakala, Int. J. Inorg. Chem., **13**, 1 (2013).
7. F. Mo, G. Dong, Y. Zhang and J. Wang, Org. Biomol. Chem., **11**, 1582 (2013).
8. S. M. Abdallah, Arab. J. Chem., **5**, 251 (2012).
9. H. M. Killa, E. M. Mabrouk, A. A. Abd El-Fattah and S. A. Yasen, Anal. Lett., **24**, 275 (1991).
10. P. Mangaiyarkkarasi and S. A. Antony, J. Appl. Chem., **3**, 997 (2014).
11. A. Singh, R. Choi, B. Choi and J. Koh, Dye Pigment., **95**, 580 (2012).
12. A. Ravindran, P. Chandran and S. S. Khan, Colloids Surf. B. Biointerfaces, **105**, 342 (2013).
13. H. J. Mohammed, A. Y. Muhi and H. Al Meisslemaw, E-J. Chem., **8**, S425 (2011).
14. C. Ruffert, N. C. Bigall, A. Feldhoff and L. Rissing, IEEE Trans. Magn., **50**, 1 (2014).
15. J. Luo, X. Dai, S. Bai, Y. Jin, Z. Ye and X. Guo, Nano-Micro Lett., **5**, 274 (2013).

*Accepted : 07.07.2015*